



Article

Remediation of Water Using a Nanofabricated Cellulose Membrane Embedded with Silver Nanoparticles

Salma Shad ^{1,2} , Iseult Lynch ^{3,*} , Syed Waqar Hussain Shah ² and Nadia Bashir ²¹ Department of Chemistry, Faculty of Natural Science, The University of Haripur, Haripur 22620, Pakistan² Department of Chemistry, Hazara University, Mansehra 21300, Pakistan³ School of Geography, Earth and Environmental Sciences, University of Birmingham, Edgbaston, Birmingham B15 2TT, UK

* Correspondence: i.lynch@bham.ac.uk

Abstract: The removal of pesticide pollution is imperative, because of their high environmental load and persistence, and their potential for bioaccumulation in, and toxicity to the environment. Most pesticides are found to be toxic even at trace levels. AgNPs can be effectively used for the adsorption of pesticides, and the incorporation of the AgNPs onto a support polymeric membrane enhances their effectiveness and reduces the potential unwanted consequences of intentionally adding free nanoparticles to the environment. Here, silver nanoparticles (AgNPs) were synthesized using a reliable, eco-friendly, and one-step “green” method, by reacting *Mentha Piperita* (mint) extract with AgNO₃ aqueous solution at 60 °C in a microwave. The resulting high surface area nanoparticles are both economic and effective environmental remediation agents, playing a promising role in the elimination of aquatic pesticide pollution. Embedding the nanoparticles into a cellulose membrane at a low concentration (0.1 g) of AgNPs was shown to result in effectively adsorption of representative pesticides (Cypermethrin, Paraquat, and Cartap) within 60 min, while increasing the concentration of nanoparticles incorporated into the membrane further enhanced the removal of the exemplar pesticides from water. The high adsorption capacity makes the cellulose-AgNPs membrane an excellent substrate for the remediation of pesticide-polluted water.

Keywords: pesticide contamination; nanoparticle-enhanced polymeric membrane; adsorption; remediation; agricultural run-off



Citation: Shad, S.; Lynch, I.; Shah, S.W.H.; Bashir, N. Remediation of Water Using a Nanofabricated Cellulose Membrane Embedded with Silver Nanoparticles. *Membranes* **2022**, *12*, 1035. <https://doi.org/10.3390/membranes12111035>

Academic Editor: Ahmad Fauzi Ismail

Received: 3 September 2022

Accepted: 17 October 2022

Published: 24 October 2022

Publisher's Note: MDPI stays neutral with regard to jurisdictional claims in published maps and institutional affiliations.



Copyright: © 2022 by the authors. Licensee MDPI, Basel, Switzerland. This article is an open access article distributed under the terms and conditions of the Creative Commons Attribution (CC BY) license (<https://creativecommons.org/licenses/by/4.0/>).

1. Introduction

Pesticides are well-known environmental pollutants, with many possessing mutagenic properties leading to induction of mutations, chromosomal alterations or DNA damage, adversely affecting ecosystems and humans. According to the World Health Organization (WHO), based on a systematic review of reporting data from 141 countries from 157 articles and data from the WHO Mortality Database, approximately 740,000 annual cases of UAPP were reported with about 10% of these resulting in fatalities. Scaling this up, leads to an estimate of 385 million cases of pesticide poisoning annually world-wide [1]. Occupational exposures and work-related contact with pesticides account for 70% of the mortalities, and chronic exposure is associated with a group of syndromes, including numerous tumors and nervous system disorders [2]. Insecticides mostly target the nervous system including the acetylcholine receptor (e.g., a target for neonicotinoids) and acetylcholinesterase, an enzyme which plays an important role in the mediation of nerve impulses [3].

Despite their purpose in killing pests, insecticides and herbicides have been allowed for restricted use to control pests or weeds in agriculture, with restrictions including the amounts, rates of applications and crops on which they can be applied, and as data accumulates on their hazards some are banned outright [4]. Besides agriculture, pesticide control is essential in dwellings, laboratories, and food processing installations. Significantly, these

chemicals are often human carcinogens, with exposure via ingestion, absorption through the skin, or inhalation, and their long-term exposure may prove fatal [5]. Hence, minimizing pesticide usage and eliminating their excess run-off in the environment is desirable. However, the high binding affinity of soil serves as a storehouse of pesticides and the metabolites [6,7]. Water resources are susceptible to pesticide contamination because of the close interconnection of soil and water bodies. The assimilation of contaminated water can mimic the human body's hormones that reduce immunity and prevent chronic and reproductive issues [8].

Cypermethrin (CP), a synthetic pyrethroid, and Cartap (CA) a thiocarbamate insecticide inhibit the nervous system of insects, causing paralysis and eventual death [8,9]. CA has been identified as a toxic pollutant, inducing endocrine disruption, neurotoxicity, and can also affect carbon and nitrogen fixation of cyanobacteria [9]. Highly reactive free radicals are generated during the utilization of Paraquat (PQ), which leads to lipid peroxidation, membrane damage and cell death in plants and mammals. PQ is mainly absorbed orally and via inhalation by animals and becomes highly concentrated in kidneys and lungs [10]. The structures of the herbicides/insecticides used in the present study are provided in Figure 1. Based on the toxicological effects of these pesticides, their widespread use globally, and their range of physicochemical properties (see Table 1), the assessment of their removal from water using sustainable and low-cost approaches is of great interest.

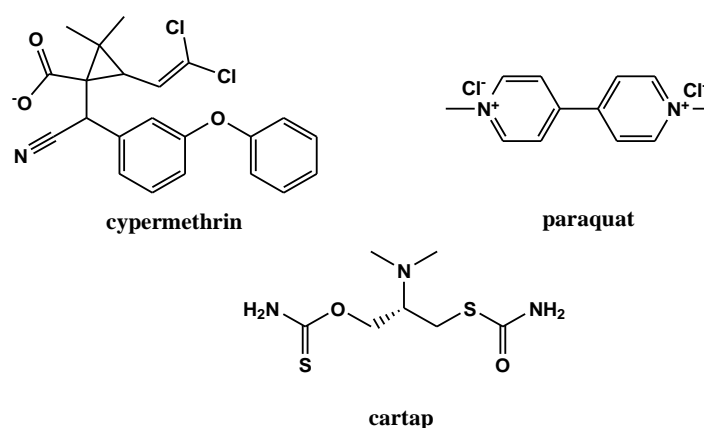


Figure 1. The chemical structures of the tested pesticides—Cypermethrin (CP), Paraquat (PQ), and Cartap hydrochloride (CA).

Table 1. The various properties and harmful effects of the pesticides utilized in this study.

Herbicide/ Insecticide	Use	Approval	Toxicity Threshold		Log K_{ow}	LD ₅₀
			Human	Marine life		
Cypermethrin (CP)	Insecticide for cotton, fruits, and vegetables, Commercial and residential settings	EPA, US for restricted control of insects	Long-term, High	Extra high for fish	>4.5 (bioaccumulation expected)	57,500 µg/kg (oral, rat)
Cartap hydrochloride (CA)	Targets chewing and sucking insects on many crops, including rice.	1967 Japan, US Chewing and sucking pests	Long-term, very low	Long-term, very low	0.0	250–340 mg/kg (oral, rat)
Paraquat (PQ)	Herbicide for weeds and grasses in agricultural & non-agricultural areas	EPA, US restricted use of pesticide	Long-term, high	Not available	−4.0 (unlikely to bio accumulate)	110–150 mg/kg (rats)

The development of low-cost solutions for the removal of pesticides from aquatic systems is an active research field, with a range of techniques suggested for removal

of pesticide contaminants including hydrogen peroxides, ultrasonic waves, hybrid processes, bioremediation, photocatalytic degradation, adsorption, membrane separation, bio-purification systems, composite materials, ion exchange resins, carbon nanotubes, graphene, and nanocrystalline metal oxides [11]. For example, nanoparticles (NPs) formed by noble metals such as silver can be harnessed for remediation of agricultural soils and contaminated water bodies, owing to their ability to bind and degrade pesticides [12]. NPs have gained immense interest for use in biomedicine, drug delivery, optoelectronics, catalysis, optics, and environmental protection [13,14]. Several physio-chemical techniques have been extensively employed for AgNPs synthesis such as microwave, sonochemical, hydrothermal, wet chemical, sol-gel, etc., but have some disadvantages such as the usage of high beam energy, toxic wastes, high costs, and toxic byproducts production, causing severe environmental contamination [15,16]. To overcome these limitations, development of eco-friendly techniques is needed. Green or sustainable chemistry is the chemical philosophy that encourages the design of products and processes which eliminate the use or generation of hazardous substances [17]. One such approach is the exploitation of biological molecules for the synthesis of NPs using biomolecules as reducing and capping agents for NPs [16,18]. Through the green approach, NPs generally have a broad size distribution, because of the presence of several reducing species and a variety of capping agents in an extract, which necessitate control and optimization [16–20]. Another green approach involves the use of microwave-assisted reactions (MAR), which supports the biosynthesis of NPs by providing the high temperature needed for the nucleation process, thereby enhancing the reaction kinetics and reducing the reaction times and associated energy costs [21–23]. NPs produced through microwave heating have excellent crystallinity as microwaves provide great control over the morphology and shape of the nanostructured particles [21].

AgNPs synthesized by the green method have been successfully employed in numerous pharmaceutical and biomedical fields due to their high chemical stability [24,25]. AgNPs absorb and scatter light with extraordinary efficiency due to localized Plasmon, with the interaction of electromagnetic waves leading to localized Plasmon resonance. Furthermore, the absorption and scattering properties of NPs could be altered by controlling the particle size, crystal shape, and refractive index [26,27]. NPs provide a highly effective solution to clean up the environment and support remediation by acting as a chemical reductant. Their capacity to adsorb biomolecules and interact with biological receptors means that NPs can reach sub-cellular locations, leading to potentially higher localized concentrations of ions once those particles start to dissolve or degrade in situ [28]. AgNPs are used in several consumer products, whereby significant amounts go down the drain and are eventually released into the sewer system and reach wastewater treatment plants. Through waste treatment, NPs are converted into free silver ions, agglomerate, or interact and complex with ligands such as sulfides present in sludge and effluent [29–31]. These environmental transformations can affect the properties of the suspended NPs that result in changes in their aggregation or oxidation states, precipitation of secondary phases, or sorption of organic species, resulting in the formation of colloidal solutions that are potentially toxic [32]. Thus safe use of NPs for environmental applications, such as adsorption and removal of pesticides due to enhanced reactivity, many edges, and high-energy surface defects [33], requires understanding of their environmental transformations.

Composite membranes functionalized with NPs have been shown to remove contaminants from water due to their binding ability through ultra-, micro- and nano-filtration, and reverse osmosis [34–36]. Fabrication of membranes that entrap the NPs reduces the risks of NPs addition into and transformation by the environment, and can also prevent biomolecule fouling of the membrane due to the accumulation of salts, colloids, and macromolecules [37]. The antimicrobial properties of AgNPs can reduce the membrane biofouling, thus providing a win-win low-cost solution [38]. The dense nano-pores of microfiltration (MF) membranes, with a microporous structure such as cellulose filter paper, have drawn increasing interest as a means to remove colloids and suspended solids effectively from drinking water sources [39,40]. With efficient antibacterial activities, AgNPs are actively

used in MF membrane preparation with noncovalent interactions between NPs and the membranes [41–48]. In many cases, the leaching of AgNPs into treated drinking water will be inevitable, which is a potential threat to both humans and the environment [49,50]. The fabrication of AgNPs into cellulose acetate membranes makes the surface more hydrophilic by allowing an increase in the flux that permeates the membrane [42]. A polymer such as cellulose acetate is preferred in water remediation technologies because of its net negative surface charge that allows control over biofouling. Besides, cellulose acetate membranes are biodegradable, resistant to chlorine, hydrophilic, renewable, and inexpensive [41–48].

In the present work, AgNPs were synthesized by reducing Ag ions in an aqueous solution of mint extract with the precursor salt of silver nitrate (AgNO_3). With the presence of chemical constituents (terpenoids, flavonoids, phenolic acid, polyphenols, proteins, sugar, etc.) in the plant extract, reduction occurs. The multifunctional AgNPs were characterized and fabricated into the composite cellulose acetate membrane. The efficiency of the AgNPs and composite membrane for the removal of organic pollutants were studied. The process was optimized to eliminate any inherent shortcomings and presents the first evidence of the effectiveness of these low-cost sustainable AgNPs-cellulose acetate membranes at removing pesticides from drinking water.

2. Materials and Methods

2.1. Materials

Silver nitrate (AgNO_3) and cellulose acetate were purchased from Sigma-Aldrich (Merck KGaA, Darmstadt, Germany). Herbicides (CP & PQ) and an insecticide, cellulose acetate (CA) was purchased from Merck (Sigma-Aldrich, Darmstadt, Germany). Methanol, ethanol (99% purity, Merck, Sigma-Aldrich) and acetone (100% pure) used in the work were of high purity and analytical grade. All chemicals were utilized as received.

2.2. Green Synthesis of Silver Nanoparticles

The plant extract was prepared according to the procedure reported elsewhere [21]. Briefly, twenty milliliters (20 mL) of filtrate of *Mentha* leaf extract was mixed with 5 mM silver nitrate solution in a 1:2 *v/v* ratio at 60 °C and heated using a microwave (INPUT: 230–240 V~50 Hz 1200 W (MICRO), OUTPUT: 700 W 2450 MHz (Boss international company)) set at 48 °C. A visible brown color change occurred within 2 min, which indicated the formation of NPs. Un-aggregated AgNPs gave a yellow color to the solution. The solution was centrifuged for 20 min at 5000 rpm and decanted at room temperature. The residual supernatant was removed by using a pipette, and the solid pellet was washed with deionized water. Further purification was carried out by centrifugation at 15,000 rpm for 20 min. This process was repeated at least three times, and the lower pellet was collected and dried at 60 °C in an oven. The dried pellet was then transferred to an airtight vial and kept in the dark for further use. The synthesis time was optimized from 1 to 10 min and analysis was done by using a UV/Visible spectrophotometer. At the heating time duration of 2 min, higher absorbance and better productivity of nanoparticles were optimized as shown in Figure 2b.

2.3. Fabrication of AgNPs and Composite Membrane

2.5 g of cellulose acetate was dissolved in 50 mL of acetone and stirred until complete dissolution. To this solution, the selected amount of AgNPs was added with stirring to form a homogeneous mixture. To be comparable with the free NP adsorption studies, we added 0.1 mg AgNPs to the cellulose acetate solution. The viscous solution thus obtained was cast onto a dry glass plate for film formation. The thin film was air-dried for 30 s and then immersed in 100% pure ethanol until needed. A similar method was repeated for the preparation of a blank membrane without the addition of AgNPs. Later, a 2 cm piece of the fabricated membrane was cut and used for the removal of contaminants [21].

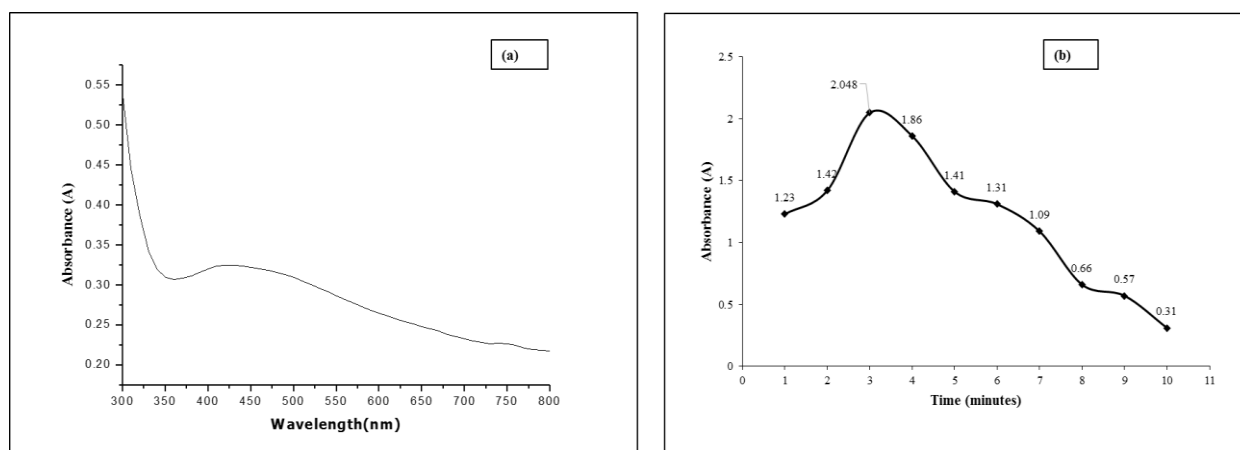


Figure 2. (a) The surface plasmon absorbance spectrum of the 20 nm AgNPs produced using the optimized conditions: (b) Effect of exposure time on the synthesis of nanoparticles using microwave (MW) irradiation determined at 425 nm.

2.4. Characterization of Biosynthesized Nanoparticles and Composite Membrane

All characterization was performed at the School of Geography, Earth, and Environmental Sciences, University of Birmingham. The reduction of silver ions by plant extract was followed by recording time-dependent absorbance using a Perkin Elmer Lambda-25 UV-Visible Spectrophotometer. The size distribution was analyzed by nanoparticle tracking analysis (NTA) using a Nano Sight (LM-20). Elemental analysis was done through energy dispersive x-ray (EDX) spectroscopy. Zeta potential, particle size, and the stability of AgNPs were determined through dynamic light scattering, DLS (Zeta sizer Nano series). Silver nanoparticles were studied on carbon-coated copper grids and analyzed using a JEM 1400 Transmission Electron Microscope (TEM) operating at a voltage of 80 kV. About 500 nanoparticles were studied by using Image J software to measure the size of the AgNPs. X-ray diffraction (XRD) analysis was performed by X-ray Diffractometer Model Analytical X-pert Pro to study the structure and shape of NPs. Atomic force microscopy (AFM) was harnessed for analysis of the AgNPs-cellulose acetate composite membrane thickness and surface roughness, as well as to monitor the removal of pesticide/insecticide by binding to the membrane surface.

2.5. Efficiency of Biogenic AgNPs for Adsorption of Insecticides and Herbicides from a Contaminated Water Sample

The adsorption/removal of pesticides from the water samples was studied using the AgNPs added directly to the water sample and using the AgNPs-cellulose acetate membrane with a comparable total amount of AgNPs. Pesticide solutions of 1 ppm, 5 ppm, and 10 ppm concentrations were prepared.

(1) Treatment with Silver Nanoparticles

A fixed amount (0.1 mg) of the dried AgNPs was added to each (1 ppm, 5 ppm & 10 ppm) herbicide/insecticide solutions. The pH and time-dependent absorbance (A) were studied at the maximum absorbance wavelength for each analyte ($\lambda = 617$ nm with $A = 0.031$ for CP, $\lambda = 320$ nm with $A = 0.037$ for CA, and $\lambda = 408$ nm with $A = 0.191$ for PQ, respectively) were recorded. The effect of variation of the initial pesticide concentration (at a constant AgNPs concentration) was also determined.

(2) Treatment with Composite Membrane

The nanofabricated composite membrane was cut into small pieces (2 cm) and dipped into the pesticide solutions (CP, CA, and PQ) at room temperature. The time-dependent absorbance was measured every 120 s (2 min) over 60 min to follow the entrapment/mineralization of the contaminant onto the AgNPs-loaded membrane. The absorbance was recorded at 617 nm,

320 nm, and 408 nm for CP, CA, and PQ, respectively. The adsorption capacity of the nanocomposite membrane was determined using Equation (1) as follows:

$$q_e = \frac{C_0 - C_e}{M} \times V \quad (1)$$

where C_e and C_0 are the pesticide concentrations at equilibrium and initial conditions (mg L^{-1}), respectively. The parameter of M is the mass of AgNPs (g) and V (L) is the volume of the solution. The percentage of pesticide adsorption (% adsorption) was calculated by Equation (2) as follows:

$$R = \left(1 - \frac{C_0}{C_e}\right) \times 100 \quad (2)$$

All adsorption experiments were conducted in triplicate, and the mean and average values of the three runs are reported. Adsorption was evaluated as a function of time at varied CP concentrations (1 ppm, 5 ppm & 10 ppm), with an adsorbent dose of 0.1 g AgNPs, and a volume of CP solution of 100 mL, based on the amount of CP remaining in solution over time; thus, a decrease in CP concentration correlates with CP adsorption on the AgNPs surface and its removal from the water.

3. Results

3.1. UV-Visible Analysis of the Synthesized Nanoparticles

The UV-visible absorption spectrum of the biosynthesized AgNPs is shown in Figure 2a, and the corresponding time-dependent change in absorbance at 425 nm due to microwave exposure is shown in Figure 2b. The maximum intensity was obtained at an MW-exposure (60°C) time of 3 min, indicating the completion of chemical conversion to zero-valent silver NPs [27]. However, no leveling off effect is observed at higher exposure times, which reveals further morphological or chemical changes occurring in the system.

The formation of the AgNPs is confirmed by a change in the color over the reaction duration due to excitation of surface plasmon vibrations [27], and the optimal synthesis time was selected as 3 min for the subsequent studies, as reaction time has been identified as one of the factors affecting the yield of AgNPs. The UV-Visible absorbance was recorded after different heating time intervals from 1 min to 10 min from the initiation of the reaction. The visual (brown color) observation and UV-Vis spectra revealed that the formation of AgNPs occurred within three minutes.

3.2. Transmission Electron Microscopy (TEM) and Dynamic Light Scattering (DLS) Analysis

The size, shape, and morphology of the AgNPs synthesized were determined through TEM, and the resulting image is shown in Figure 3a. The heterogeneity in the size of the NPs is visible and reveals that NPs are well dispersed and spherical (shape), while some have irregular structures. However, image J analysis indicated that greater than 80% of the particles had a size (diameter) in the range of 15–20 nm. The image analysis also indicates negligible agglomeration, which is expected, considering the variety of chemical species present in leaf extract that act to stabilize nano-sized metal clusters, as shown in Figure 3b. The DLS and Nanoparticle tracking analysis (NTA) data confirm the particle size and dispersion characteristics (Figure 4b,c) and the particles are found to be slightly positively charged (Figure 4a).

3.3. X-ray Diffraction (XRD) Analysis of AgNPs

Figure 5 depicts the XRD pattern of the synthesized AgNPs. Typical peaks at 32.50° , 38.36° , 44.56° , 64.81° , and 77.66° were assigned to (100), (200), (220), (111), and (311) planes and compared with the standard powder diffraction card of JCPDS (File No. 04-0783) that confirmed the presence of silver ions and the crystalline nature of the synthesized AgNPs. No peaks were observed that would correspond to the presence of impurities. XRD revealed the monoclinic structure of the synthesized AgNPs.

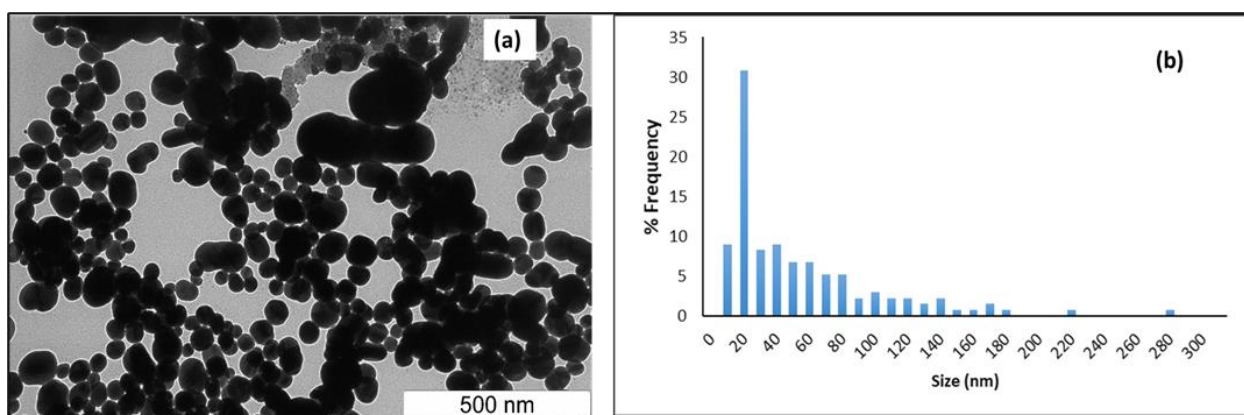


Figure 3. (a) TEM image of AgNPs (b) Histogram of Image J excel result of synthesized Ag nanoparticles.

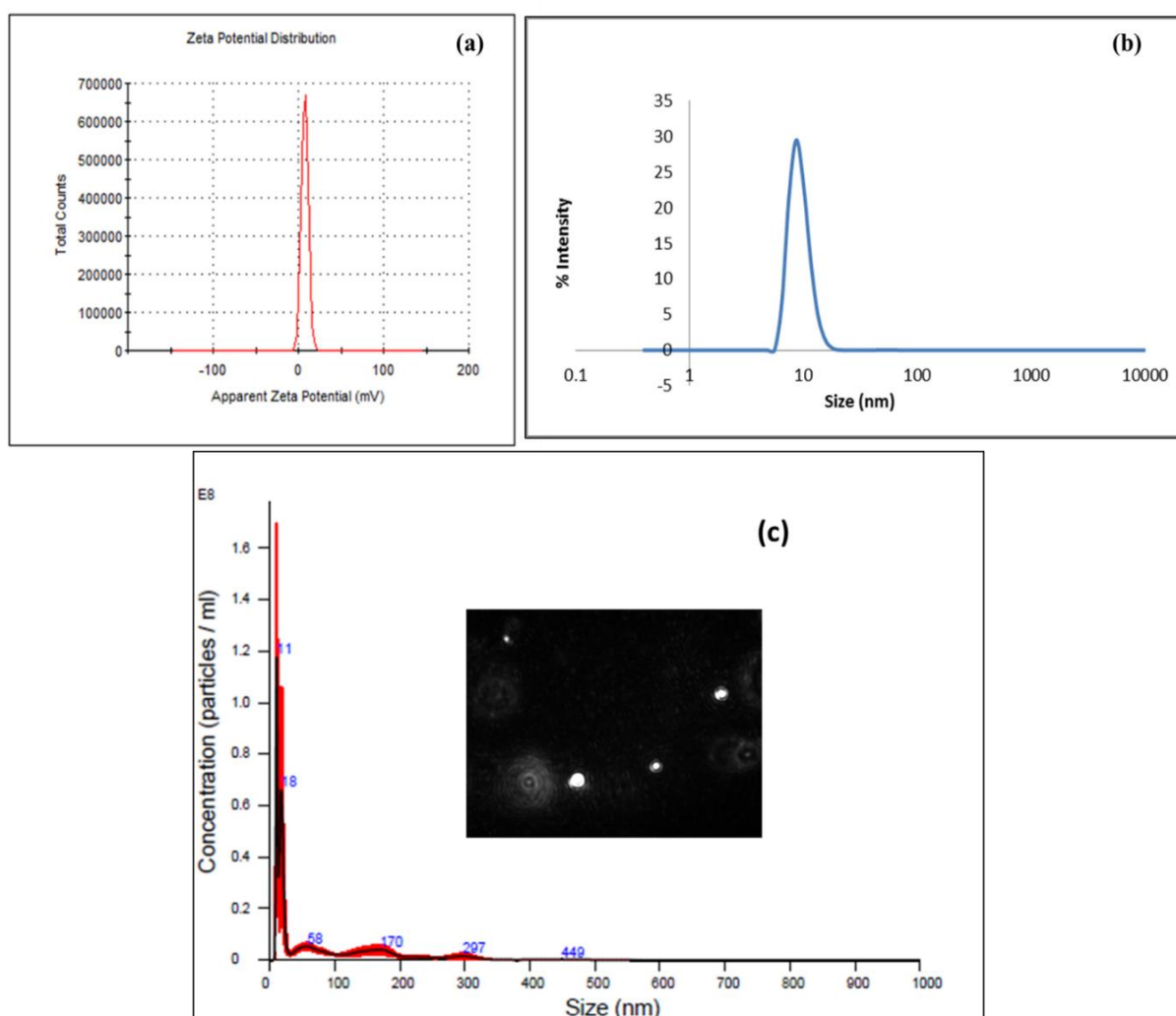


Figure 4. (a) Zeta potential of AgNPs by DLS, (b) Histogram showing the calculated particle size of AgNPs by DLS (c) Nanoparticle tracking analysis showing the Brownian motion of AgNPs, and that most of the particles are <30 nm.

3.4. Atomic Force Microscopy (AFM) Analysis of AgNPs Formation

Figure 6 depicts a 3D AFM image of the AgNPs, and the brighter spots confirm the location of the NPs due to their high modulus as compared to the mica surface. Further, it is confirmed that the AgNPs are of uniform size and are spherical. An XE-100 Advanced

Scanning Probe Microscope was used to study the surface roughness of the NPs before and after embedding them into the cellulose acetate membrane. There were no signs of aggregation with the naked eye, indicating that NPs were well dispersed throughout the polymeric matrix.

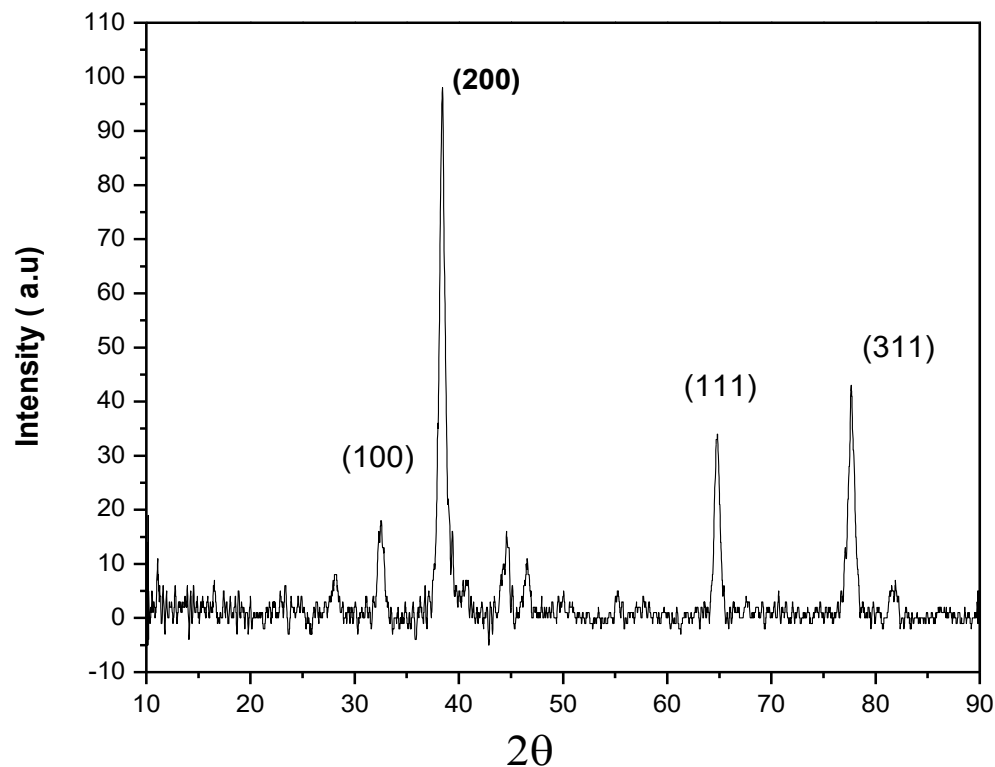


Figure 5. XRD analysis of the free AgNPs.

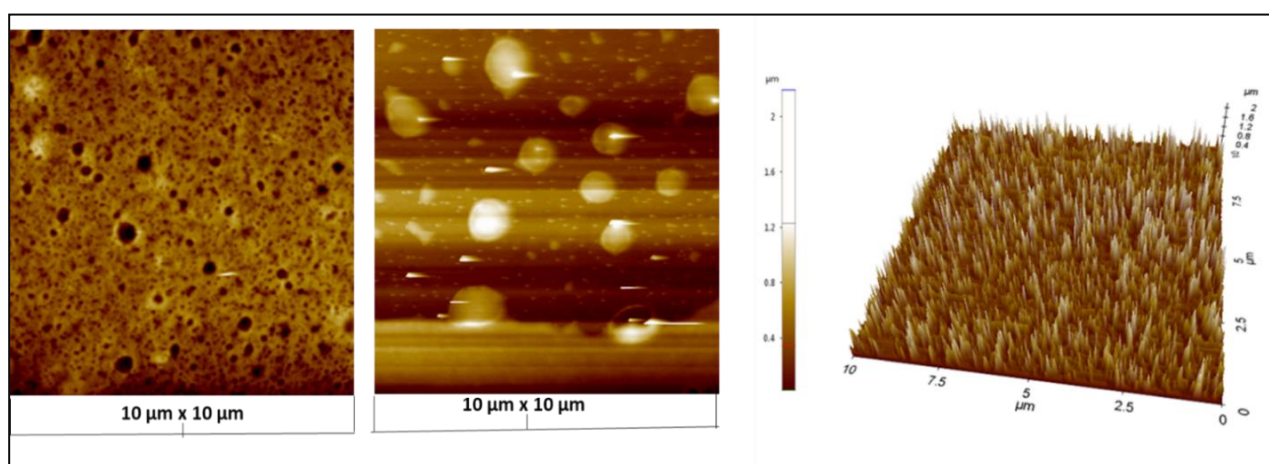


Figure 6. AFM analysis of AgNPs and 3D magnification over $10\ \mu\text{m} \times 10\ \mu\text{m}$.

3.5. Incorporation of Ag Nanoparticles into the Cellulose Acetate Membrane

To assess sample uniformity, topography and other surface properties were studied over a larger area at various locations. Smaller sections were scanned at higher resolution. The surface roughness and porosity of the cellulose acetate membrane were found to be altered by incorporation of the AgNPs—pores of micrometer size were formed after incorporation of NPs into the membrane, as represented in the 3D image of AFM (Figure 7a), while the surface roughness of the membrane was not changed by the modification with AgNPs.

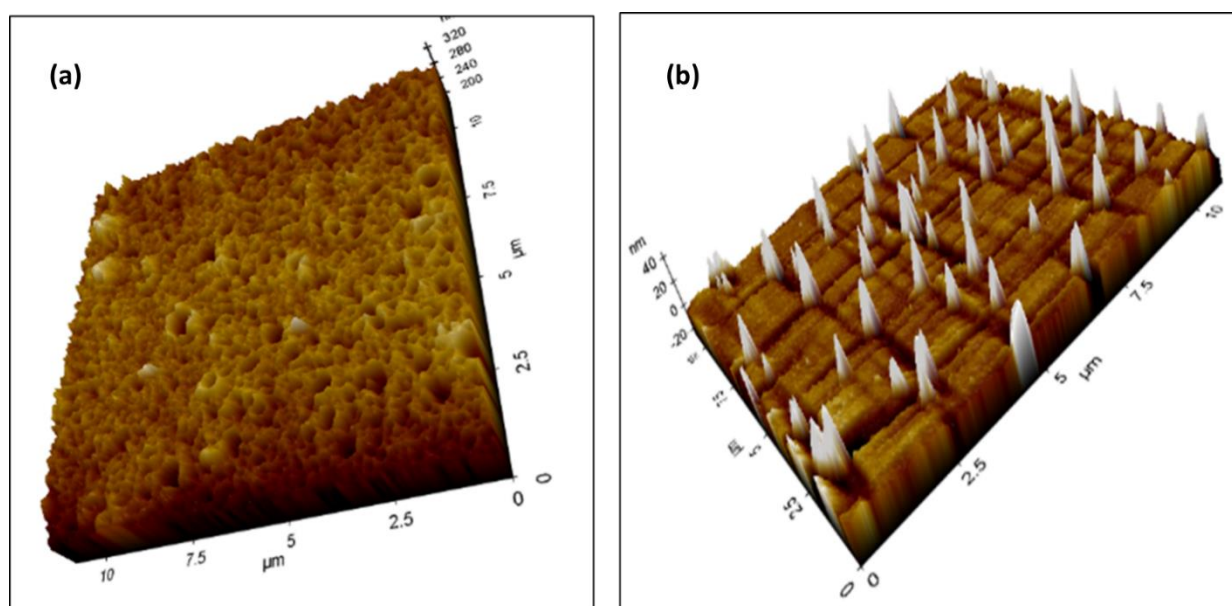


Figure 7. 3D images via AFM analysis (a) Illustration of the porosity and (b) dispersion of AgNPs throughout the polymeric matrix, scanning over a $10\ \mu\text{m} \times 10\ \mu\text{m}$ area.

3.6. Removal of Cypermethrin from Water Using AgNPs and Cellulose Acetate Membrane Incorporated with AgNPs

Both CP and CA belong to the well-known nereistoxin insecticidal class of pesticides, which act by blocking the nicotinic acetylcholine receptor. The interaction of these pesticides with NPs results in binding of the pesticide to the reactive surface of the NMs, potentially displacing some of the mint extract components, or binding to them [51–53]. The adsorption of pesticides on AgNPs was first followed spectrophotometrically, while NPs can be spread homogeneously on the substrate, so the fraction of surface atoms becomes large. At a constant concentration of 0.1 g AgNPs/100 mL of the CP solution, and thus a constant surface area for binding, the removal of pesticide at room temperature was observed. Increasing the concentration of CP from 1 ppm to 5 ppm and 10 ppm resulted in decreased CP removal efficiency due to saturation of the binding sites. The decreased percent removal with an increase can be explained by the fact that the active sites of AgNPs become saturated above a certain concentration. The absorbance intensity of the solution decreases as the concentration of pesticide decreases because of binding to the AgNPs, which removes the pesticide from the solution; at higher initial CP concentrations (5 ppm, and 10 ppm) a very rapid initial decrease is observed within the first 10 min due to the availability of more active sites, followed by a slower removal phase over the subsequent 20–60 min, as shown in Figure 8.

The AgNPs showed a promising result by absorbing 93.9% of CP from a 1 ppm solution within 60 min. At a higher concentration of the insecticidal solution and a constant AgNPs concentration, the AgNPs absorbed 68.8% of the 5 ppm solution with the first 60 min, and 20.02% of the 10 ppm solution in less than 3 min. It was found that the AgNPs showed a promising result in the removal of insecticide. As shown in Figure 8, adsorption started rapidly and reached a plateau within 20 min, which could be related to the availability of more binding sites at the beginning, which became saturated with time, and second, a gradual decrease in the concentration gradient between the bulk solution and adsorbent was evident. Similarly, with unchanged adsorbent mass and volume, the ratio of active sites to the ions of CP became lower at a higher initial concentration, which led to a decrease in the percentage of removal.

To assess the impact of stabilizing the AgNPs into a cellulose acetate membrane, a small portion (2 cm) of polymeric membrane incorporated with 0.1 g of AgNPs was

cut and immersed into the samples containing the CP insecticide. After immersion of the membrane, 2 mL of the solution was checked by a UV/Visible spectrophotometer. The AgNPs polymeric membrane gave an excellent result, by adsorbing 99.8% of 1 ppm insecticide (CP) solution, due to the availability of more surface area, within the time duration of only 20 min. While in the case of 5 ppm and 10 ppm, the membrane took 30 to 35 min for the adsorption of essentially all available CP. The same studies were carried out with the blank membrane prepared without incorporation of AgNPs, whereby it was observed that within the first five minutes the blank membrane reaches a constant absorption level with no change in the value after the initial 5 min.

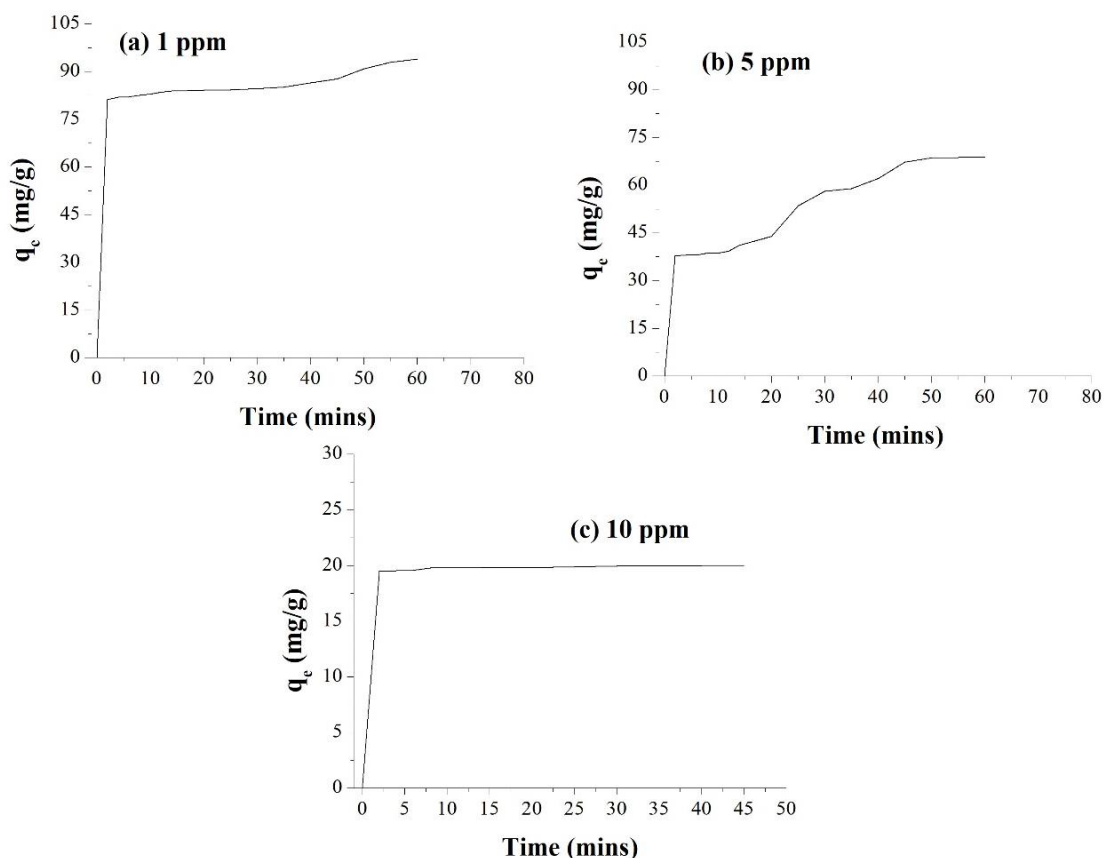


Figure 8. % Adsorption of the insecticide CP by free AgNPs at different initial AgNPs concentrations.

The results shown in Table 2 demonstrate that the AgNPs individually adsorbed 93.9% of CP from the 1 ppm water sample within 60 min while AgNPs showed better adsorption after fabrication into the polymeric membrane. After fabrication into the polymeric membrane, not only was the time of adsorption reduced but also effectiveness increased as determined by the increased % adsorption of CP.

Table 2. % Adsorption of Cypermethrin (CP) insecticide by free AgNPs and AgNPs incorporated into a cellulose membrane, as a function of the initial insecticide concentration.

	Adsorption of CP by 0.1 g AgNPs			Adsorption of CP by 0.1 g AgNPs Incorporated into the Cellulose Membrane			Adsorption with the Membrane (without AgNPs)
	1 ppm (CP)	5 ppm (CP)	10 ppm (CP)	1 ppm (CP)	5 ppm (CP)	10 ppm (CP)	
% Adsorption	93.9	68.8	20.02	99.8	97.9	95.1	0.6
Adsorption Time (min)	60	60	60	20	30	35	60

3.7. Removal of CA and PQ by Using AgNPs and Membrane Incorporated with AgNPs

Figure 9 represents the time-dependent removal of CA at different concentrations at constant NP concentration. It is concluded that the time taken for removal increases as the pesticide concentration increases, due to the limited number of sites for absorption, and that the number of active sites determines the rate of pesticide removal.

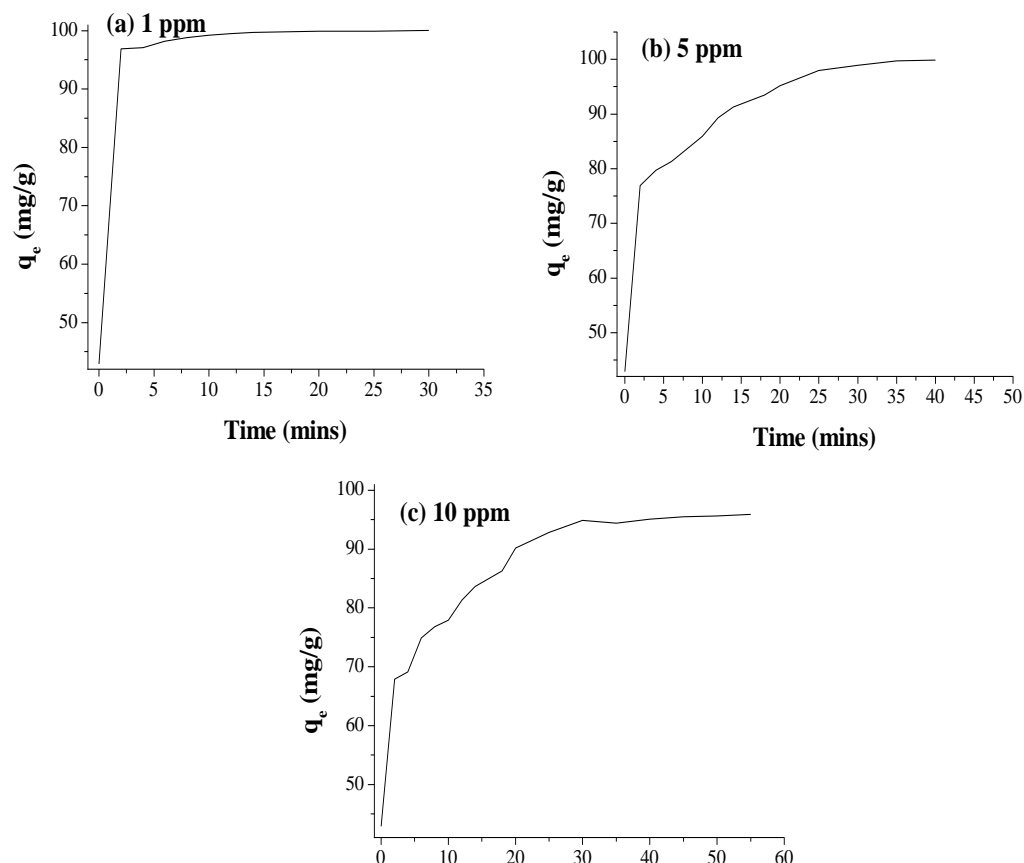


Figure 9. % Adsorption of CA from water by free AgNPs at different initial AgNPs concentrations.

By applying the kinetics equations, it is concluded that 100% of CA insecticide was adsorbed by the AgNPs incorporated membrane within 60 min. In the case of CA, the membrane was found to be effective and efficient enough to remove 99.9% of insecticide of different concentrations from the water sample within 20–45 min, as shown in Table 3.

Table 3. % Adsorption of Cartap (CA) by free AgNPs and AgNPs incorporated into a cellulose acetate membrane, at different initial concentrations of the insecticide.

	Adsorption by 0.1 g AgNPs			Adsorption of CP by 0.1 g AgNPs Incorporated into the Cellulose Membrane			Adsorption with the Membrane (without AgNPs)
	1 ppm (CA)	5 ppm (CA)	10 ppm (CA)	1 ppm (CA)	5 ppm (CA)	10 ppm (CA)	
% Adsorption	100	79.1	66	100	91.2	89.7	0.5
Adsorption Time (min)	35	60	60	20	35	45	60

A similar study was conducted for the removal of PQ herbicide from the water sample using AgNPs and a fabricated polymeric membrane. The synthesized AgNPs adsorbed 91.9% to 98.9% PQ herbicide with the same time duration (60 min), as confirmed in Figure 10. Again, the AgNPs incorporated membrane showed its efficiency by minimizing the time

of adsorption by adsorbing 100% of 1 ppm PQ from water in no more than 20 min, as shown in Table 4. The blank membrane has shown no prominent role in the absorption efficiency for the respective herbicide, reaching saturation at a low level of adsorption after five minutes of exposure.

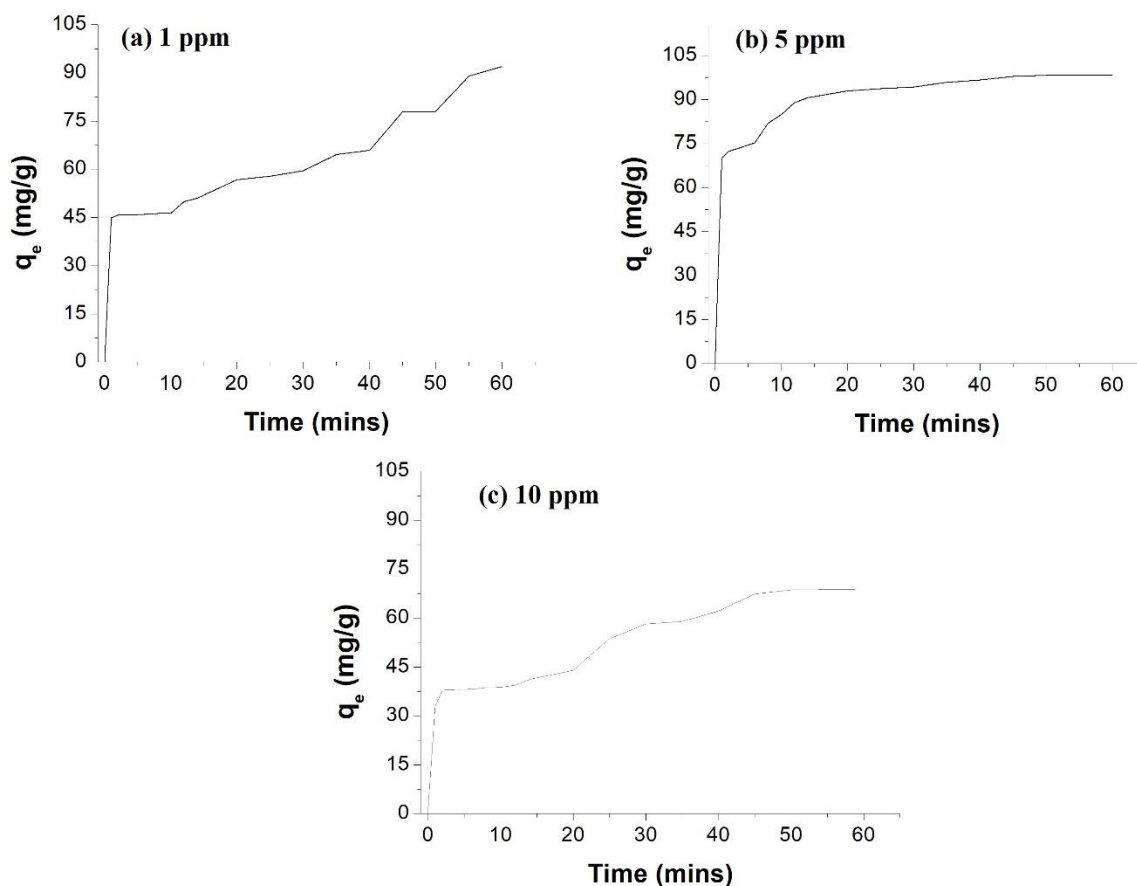


Figure 10. % Adsorption of PQ herbicide from water by free AgNPs at different initial AgNPs concentrations.

Table 4. % Adsorption of Paraquat (PQ) by free AgNPs and AgNPs incorporated into the cellulose acetate membrane with different initial insecticide concentrations.

	Adsorption by 0.1 g AgNPs			Adsorption by 0.1 g AgNPs Incorporated into the Cellulose Membrane			Adsorption with the Membrane (without AgNPs)
	1 ppm (PQ)	5 ppm (PQ)	10 ppm (PQ)	1 ppm (PQ)	5 ppm (PQ)	10 ppm (PQ)	
% Adsorption	93.5	51.3	73.2	100	96.5	92.7	0.7
Adsorption Time (min)	60	60	60	25	30	30	60

4. Discussion

AgNPs are one of the mostly intensively explored nanostructures due to their unique physicochemical properties and widespread biomedical applications as catalysts and as antimicrobial agents [47]. Recently, green approaches for the synthesis of NPs are becoming increasingly accepted due to the availability of a vast array of biological resources, the ability to produce high density of NPs, the stability of the resulting NPs, the decreased time requirement, and the ready dispersibility of the prepared NPs [48]. Metallic NPs have a unique catalytic activity in the degradation of halocarbons and other organic molecules,

as well as inorganic contaminants. Membranes are considered to play a pivotal role in these degradative processes by giving support for the NPs dispersion [49]. NPs incorporation into membranes has the additional advantage of decreasing chemical usage for membrane cleaning and fabrication through the antimicrobial properties of the AgNPs, thus reducing energy needs compared to conventional methods [50–53]. Yorseng et al. (2020) demonstrated that hydrothermally generated Ag NPs can be successfully utilized as a cost-effective antibacterial household cleaner and as an antibacterial filler in polymeric matrices to produce antibacterial nanocomposites [54]. NPs offer high surface area and thus numerous active sites for contaminant adsorption, while NPs incorporated into membranes show interesting properties for the removal of various trace amounts of pollutants from water by combining adsorption and filtration due to their high surface area and porosity. From an aqueous solution, the adsorbent is captured via chemical binding due to the presence of surface functional groups on the NPs, whereas physical adsorption due to van der Waals forces (porosity and high surface area of NPs) or electrostatic attraction (negatively charged nanoparticles attract positively charged metal ions) also play an important role in the binding process.

Some important information on the properties, applications, and hazards of CP, PQ, and CA is provided in Table 1. CA is a mutagenic agent, whereas CP and PQ are possible human carcinogens. Besides ingestion, they can penetrate the body through the skin and via inhalation. They attack the respiratory and central nervous systems. The bioaccumulation of CP or the logarithm of the octanol-water (ratio of chemical concentration in octanol, C_o) partition coefficient ($\log K_{ow}$) for CP exceeds +3.0, and inherent toxicity and persistence values are also high. On the other hand, the bioaccumulation of PQ is unlikely owing to the negative value of its octanol-water partition coefficient, suggesting that it prefers aquatic environments to fatty membranes.

The resulting AgNPs show a broad absorption band in the visible region of the electromagnetic spectrum, as these metal NPs show an intense color at the nanoscale which is absent in their bulk counterparts, as well as at their atomic level. The main reason behind this phenomenon is attributed to the collective oscillations of the free conductive electrons that are induced by an interaction with the electromagnetic field, known as localized surface plasmonic resonance (SPR). The presence of this band is thus used to confirm the formation of NPs and provides information on their size and shape based on the wavelength of the peak maximum and the peak shape. AgNPs SPR, and their non-bleaching properties, show significant potential for single-molecule labeling-based biological assays and near-field optical microscopic applications as a result of augmented signal output [32]. Particle size is an important property that influences the uptake and effects of NPs. Smaller particles display better antimicrobial and cytotoxic activity, as the specific surface area increases with decreasing particle size, with a greater proportion of the atoms being displayed on the surface for smaller particles. This also implies that for the same mass of NPs, biological interactions and toxicity are more dependent on particle number and surface area than on the particle mass. Additionally, the properties of AgNPs can be enhanced by NPs functionalization by different coatings and fabrication routes that influence the surface charge, solubility, and hydrophobicity, and thus the NPs binding capacity for other organic and inorganic constituents of their surroundings.

The number of pesticide molecules adsorbed by AgNPs and AgNPs incorporated into the cellulose acetate membrane was determined using the equilibrium adsorption equation. The results indicate that the main adsorption occurred as a monolayer or through the fixed number of identified active sites on the AgNPs. As reported earlier, AgNPs are an effective biocidal agent and are broadly employed for the fabrication of antifouling membranes due to their strong inhibitory and biocidal performance against various microorganisms and low toxicity toward mammalian cells for long-term applications. Both AgNPs and released Ag^+ ions can kill bacteria and prevent biofilm formation on the membrane surface; however, the AgNPs also act as a controllable source of Ag ions, demonstrating more lasting effects than Ag ions directly incorporated into the membranes. Given that the WHO have

highlighted that that too high concentrations of Ag^+ ions are harmful to human beings [55], use of the AgNP form facilitates effective slow release while maintaining the level of Ag ions below the harmful effects threshold. The AgNPs can be fixed into the membrane using a range of approaches such as surface grafting, physical blending, surface coating, and characterization of the stability of AgNPs incorporated into the membrane is important to ensure the long-term anti-biofouling property of the membrane but also to guarantee a low Ag concentration in the aqueous solution.

5. Conclusions

AgNPs were successfully synthesized from *Mentha piperita* extract and proved to be highly effective in removing pesticides from aqueous solutions. The stability of the AgNPs was confirmed by UV-Visible spectrophotometry while the SPR band was found at 425 nm. TEM images verified the formation of well-dispersed and spherical-shaped AgNPs with a mean size of 20 nm. AFM demonstrated an even distribution of AgNPs incorporation in the cellulose acetate membrane and no agglomeration was observed. The adsorption of pesticides on AgNPs and AgNPs incorporated membrane was investigated in an aqueous solution at room temperature. 0.1 g adsorbents (AgNPs) were found to be efficient and effective at lower pesticide concentrations, by removing the the maximum amount of pesticides from the water sample within 60 min, due to the presence of an optimal amount of active sites. AgNPs were successfully incorporated into the polymeric membrane and applied for the adsorption and were also shown to successfully remove the CP, CA, and PQ from the aqueous solution with an efficiency of more than 90%. Time and concentration were the main determinants of adsorption efficiency when keeping the adsorbent dosage constant. The AgNPs' incorporated membrane provides an efficient approach to completely remove 97.6–100% of the pesticides in less than 30 min. The membrane showed promising results at lower concentrations of pesticides, whereas at higher pesticide concentrations (5 ppm and 10 ppm), more saturation of active sites was observed which could potentially be overcome with higher NP loading. Hence, it can be concluded that green-synthesized AgNPs can be utilized for the effective adsorption of pesticides from contaminated water. The nano-adsorbent has been found to be very efficient and may be employed for the degradation/removal of other toxic pollutants in the future.

Author Contributions: Conceptualization, N.B.; methodology, S.S. and S.W.H.S.; formal analysis, S.S., N.B. and I.L.; investigation, S.S.; resources, I.L.; writing—original draft preparation, S.S.; writing—review and editing, I.L., S.W.H.S. and N.B.; visualization, S.S.; supervision, I.L. and N.B.; funding acquisition, S.S. and I.L.; data analysis, S.S. All authors have read and agreed to the published version of the manuscript.

Funding: Funding from the Higher Education Commission (HEC) Pakistan International Research Support Initiative Program (IRSIP) to support part of Ph.D. research to be undertaken at the School of Geography, Earth and Environmental Sciences, University of Birmingham, United Kingdom. Funding from the EU Horizon 2020 project NanoSolveIT (Grant Agreement No. 814572) is also acknowledged.

Institutional Review Board Statement: Not applicable.

Informed Consent Statement: Not applicable.

Data Availability Statement: The data presented in this study are available on request from the corresponding author.

Acknowledgments: The authors express their gratitude to the Higher Education Commission (HEC) Pakistan for granting an IRSIP Scholarship to Salma Shad and the School of Geography, Earth and Environmental Sciences, University of Birmingham, the United Kingdom for hosting Shad and their help and support in providing an opportunity to access different characterization techniques. We thank Nathan Langford, a researcher, and Marie-France Aline Belinga-Desaunay, a postdoctoral research fellow from the School of Geography, Earth and Environmental Sciences, University of Birmingham, for help and assistance in characterizations and with the AFM measurements.

Conflicts of Interest: The authors declare that they have no conflict of interest.

References

- Boedeker, W.; Watts, M.; Clausen, P.; Marquez, E. The global distribution of acute unintentional pesticide poisoning: Estimations based on a systematic review. *BMC Public Health* **2020**, *20*, 1875. [\[CrossRef\]](#) [\[PubMed\]](#)
- de Graaf, L.; Talibov, M.; Boulanger, M.; Bureau, M.; Robelot, E.; Lebailly, P.; Baldi, F.; AGRICAN group. Health of greenspace workers: Morbidity and mortality data from the AGRICAN cohort. *Environ. Res.* **2022**, *212*, 113375. [\[CrossRef\]](#) [\[PubMed\]](#)
- Scharf, M.E. Neurological Effects of Insecticides and the Insect Nervous System. In *Encyclopedia of Entomology*; Capinera, J.L., Ed.; Springer: Dordrecht, The Netherlands, 2018. [\[CrossRef\]](#)
- Donley, N. The USA lags behind other agricultural nations in banning harmful pesticides. *Environ. Health* **2019**, *18*, 44. [\[CrossRef\]](#) [\[PubMed\]](#)
- Schwingl, P.J.; Lunn, R.M.; Mehta, S.S. A tiered approach to prioritizing registered pesticides for potential cancer hazard evaluations: Implications for decision making. *Environ. Health* **2021**, *20*, 13. [\[CrossRef\]](#)
- Neuwirthová, N.; Trojan, M.; Svobodová, M.; Vašíčková, J.; Šimek, Z.; Hofman, J.; Bielská, L. Pesticide residues remaining in soils from the previous growing season (s)—Can they accumulate in non-target organisms and contaminate the food web? *Sci. Total Environ.* **2019**, *646*, 1056–1062. [\[CrossRef\]](#)
- Cardozo, M.; de Almeida, J.S.; Cavalcante, S.F.D.A.; Salgado, J.R.; Gonçalves, A.S.; França, T.C.C.; Kuca, K.; Bizzo, H.R. Biodegradation of organophosphorus compounds predicted by an enzymatic process using molecular modeling and observed in soil samples through analytical techniques and microbiological analysis: A comparison. *Molecules* **2020**, *25*, 58. [\[CrossRef\]](#)
- Vivek, C.; Veeraiyah, K.; Padmavathi, P.; Rao, D.; Bramhachari, P.V. Acute toxicity and residue analysis of cartap hydrochloride pesticide: Toxicological implications on the fingerlings of freshwater fish *Labeo rohita*. *Biocatal. Agric. Biotechnol.* **2016**, *7*, 193–201. [\[CrossRef\]](#)
- Singh, D.P.; Khattar, J.I.S.; Gupta, M.; Kaur, G. Evaluation of the toxicological impact of cartap hydrochloride on some physiological activities of a non-heterocystous cyanobacterium *Leptolyngbya foveolarum*. *Pestic. Biochem. Physiol.* **2014**, *110*, 63–70. [\[CrossRef\]](#) [\[PubMed\]](#)
- Ko, D.R.; Chung, S.P.; You, J.S.; Cho, S.; Park, Y.; Chun, B.; Moon, J.; Kim, H.; Kim, Y.H. Effects of paraquat ban on herbicide poisoning-related mortality. *Yonsei Med. J.* **2017**, *58*, 859–866. [\[CrossRef\]](#)
- Nazir, M.S.; Tahir, Z.; Hassan, S.U.; Ali, Z.; Akhtar, M.N.; Azam, K.; Abdullah, M.A. Remediation of Pesticide in Water. In *Sustainable Agriculture Reviews 47*; Inamuddin, Ahamed, M.I., Lichtfouse, E., Eds.; Sustainable Agriculture Reviews; Springer: Cham, Switzerland, 2021; Volume 47. [\[CrossRef\]](#)
- Bootharaju, M.S.; Pradeep, T. Understanding the Degradation Pathway of the Pesticide, Chlorpyrifos by Noble Metal Nanoparticles. *Langmuir* **2012**, *26*, 2671–2679. [\[CrossRef\]](#)
- Ratan, Z.A.; Haider, M.F.; Nurunnabi, M.; Shahriar, S.M.; Ahammad, A.J.; Shim, Y.Y.; Cho, J.Y. Green chemistry synthesis of silver nanoparticles and their potential anticancer effects. *Cancers* **2020**, *12*, 855. [\[CrossRef\]](#)
- Saratale, R.G.; Benelli, G.; Kumar, G.; Kim, D.S.; Saratale, G.D. Bio-fabrication of silver nanoparticles using the leaf extract of ancient herbal medicine, dandelion (*Taraxacum officinale*), evaluation of their antioxidant, anticancer potential, and antimicrobial activity against phytopathogens. *Environ. Sci. Pollut. Res.* **2018**, *25*, 10392–10406. [\[CrossRef\]](#) [\[PubMed\]](#)
- Nag, M.; Lahiri, D.; Sarkar, T.; Ghosh, S.; Dey, A.; Edinur, H.A.; Pati, S.; Ray, R.R. Microbial fabrication of nanomaterial and its role in the disintegration of exopolymeric matrices of biofilm. *Front. Chem.* **2021**, *9*, 690590. [\[CrossRef\]](#) [\[PubMed\]](#)
- Pal, G.; Rai, P.; Pandey, A. Chapter 1-Green synthesis of nanoparticles: A greener approach for a cleaner future. In *Green Synthesis; Characterization and Applications of Nanoparticles*; Micro and Nano Technologies; Elsevier: Amsterdam, The Netherlands, 2019; pp. 1–26. [\[CrossRef\]](#)
- Lahiri, D.; Nag, M.; Sheikh, H.I.; Sarkar, T.; Edinur, H.; Siddhartha, P.; Ray, R. Microbiologically synthesized nanoparticles, and their role in silencing the biofilm signaling cascade. *Front. Microbiol.* **2021**, *12*, 636588. [\[CrossRef\]](#)
- Ravichandran, V.; Vasanthi, S.; Shalini, S.; Shah, S.A.A.; Tripathy, M.; Paliwal, N. Green synthesis, characterization, the antibacterial, the antioxidant and photocatalytic activity of *Parkia speciosa* leaves extract mediated silver nanoparticles. *Results Phys.* **2019**, *15*, 102565. [\[CrossRef\]](#)
- Chinnasamy, G.; Chandrasekharan, S.; Koh, T.W.; Bhatnagar, S. Synthesis, characterization, antibacterial and wound healing efficacy of silver nanoparticles from *Azadirachta indica*. *Front. Microbiol.* **2021**, *12*, 611560. [\[CrossRef\]](#) [\[PubMed\]](#)
- Jain, N.; Jain, P.; Rajput, D.; Patil, U.K. Green synthesized plant-based silver nanoparticles: Therapeutic perspective for anticancer and antiviral activity. *Micro Nano Syst. Lett.* **2021**, *9*, 5. [\[CrossRef\]](#)
- Shad, S.; Bashir, N.; Nault, M.F.B.D.; Lynch, I. Incorporation of biogenic zinc nanoparticles into a polymeric membrane. *Clean. Eng. Technol.* **2021**, *5*, 100339. [\[CrossRef\]](#)
- Factori, I.M.; Amaral, J.M.; Camani, P.H.; Rosa, D.S.; Lima, B.A.; Brocchi, M.; da Silva, E.R.; Souza, J.S. ZnO Nanoparticle/Poly (vinyl alcohol) Nanocomposites via Microwave-Assisted Sol-Gel Synthesis for Structural Materials, UV Shielding, and Antimicrobial Activity. *ACS Appl. Nano Mater.* **2021**, *4*, 7371–7383. [\[CrossRef\]](#)
- Muzaffar, S.M.; Naeem, S.; Yaseen, S.; Riaz, S.; Kayani, Z.N.; Naseem, S. Microwave-assisted tuning of optical and magnetic properties of zinc oxide nanorods—Efficient antibacterial and photocatalytic agent. *J. Sol-Gel Sci. Technol.* **2020**, *95*, 88–100. [\[CrossRef\]](#)
- Neto, V.D.O.S.; Freire, P.D.T.C.; Nascimento, R.F.D. Removal of Pesticides and Volatile Organic Pollutants with Nanoparticle. In *Nanomaterials Applications for Environmental Matrices*; Elsevier Inc.: Amsterdam, The Netherlands, 2019; pp. 403–426. [\[CrossRef\]](#)

25. Doria, G.; Conde, J.; Veigas, B.; Giestas, L.; Almeida, C.; Assunção, M.; Rosa, J.; Baptista, P.V. Noble metal nanoparticles for bio sensing applications. *Sensors* **2012**, *12*, 1657–1687. [[CrossRef](#)] [[PubMed](#)]
26. Mendis, P.; de Silva, R.M.; de Silva, K.M.N.; Wijenayaka, L.A.; Jayawardana, K.; Yan, M. Nanosilver Rainbow: A rapid and facile method to tune different colors of nanosilver through the controlled synthesis of stable spherical silver nanoparticles. *RSC Adv.* **2016**, *6*, 48792–48799. [[CrossRef](#)]
27. Ayinde, W.B.; Gitari, W.M.; Samie, A. Optimization of microwave-assisted synthesis of silver nanoparticle by *Citrus paradisi* peel and its application against pathogenic water strain. *Green Chem. Lett. Rev.* **2019**, *12*, 225–234. [[CrossRef](#)]
28. Reidy, B.; Haase, A.; Luch, A.; Dawson, K.A.; Lynch, I. Mechanisms of silver nanoparticle release, transformation, and toxicity: A critical review of current knowledge and recommendations for future studies and applications. *Materials* **2013**, *6*, 2295–2350. [[CrossRef](#)] [[PubMed](#)]
29. Kaegi, R.; Voegelin, A.; Sinnet, B.; Zuleeg, S.; Hagendorfer, H.; Burkhardt, M.; Siegrist, H. Behavior of metallic silver nanoparticles in a pilot wastewater treatment plant. *Environ. Sci. Technol.* **2011**, *45*, 3902–3908. [[CrossRef](#)] [[PubMed](#)]
30. Hou, L.; Li, K.; Ding, Y.; Li, Y.; Chen, J.; Wu, X.; Li, X. Removal of silver nanoparticles in simulated wastewater treatment processes and its impact on COD and NH₄ reduction. *Chemosphere* **2012**, *87*, 248–252. [[CrossRef](#)]
31. Li, X.; Lenhart, J.; Walker, H. Dissolution-Accompanied Aggregation Kinetics of Silver Nanoparticles. *Langmuir* **2010**, *26*, 16690–16698. [[CrossRef](#)]
32. Gong, A.; Zhu, D.; Mei, Y.-Y.; Xu, X.-H.; Wu, F.-A.; Wang, J. Enhanced biocatalysis mechanism under microwave irradiation in isoquercitrin production revealed by circular dichroism and surface plasmon resonance spectroscopy. *Bioresour. Technol.* **2016**, *205*, 48–57. [[CrossRef](#)]
33. Wang, J.; Sui, M.; Ma, Z.; Li, H.; Yuan, B. Antibacterial performance of polymer quaternary ammonium salt-capped silver nanoparticles on *Bacillus subtilis* in water. *RSC Adv.* **2019**, *9*, 25667–25676. [[CrossRef](#)]
34. Beisl, S.; Monteiro, S.; Santos, R.; Figueiredo, A.S.; Sánchez-Loredo, M.G.; Lemos, M.A.; Lemos, F.; Minhalma, M.; de Pinho, M.N. Synthesis and Bactericide Activity of Nanofiltration Composite Membranes—Cellulose Acetate/Silver Nanoparticles and Cellulose Acetate/Silver Ion Exchanged Zeolites. *Water Res.* **2018**, *149*, 225–231. [[CrossRef](#)]
35. Raicopol, M.D.; Andronescu, C.; Voicu, S.I.; Vasile, E.; Pandeale, A.M. Cellulose acetate/layered double hydroxide adsorptive membranes for efficient removal of pharmaceutical environmental contaminants. *Carbohydr. Polym.* **2019**, *217*, 204–212. [[CrossRef](#)] [[PubMed](#)]
36. Shen, S.; Chen, H.; Wang, R. Preparation of antifouling cellulose acetate membranes with good hydrophilic and oleophobic surface properties. *Mater. Lett.* **2019**, *252*, 1–4. [[CrossRef](#)]
37. Deeksha, B.; Sadanand, V.; Hariram, N.; Rajulu, A.V. Preparation and properties of cellulose nanocomposite fabrics with in situ generated silver nanoparticles by bioreduction method. *J. Bioresour. Bioprod.* **2021**, *6*, 75–81. [[CrossRef](#)]
38. Andrade, P.F. Improved antibacterial activity of nano-filtration polysulfone membranes modified with silver nanoparticles. *Water Res.* **2015**, *81*, 333–342. [[CrossRef](#)] [[PubMed](#)]
39. Liu, G.; Yu, R.; Jiang, J.; Ding, Z.; Ma, J.; Liang, R. Robust immobilization of anionic silver nanoparticles on cellulose filter paper toward a low-cost point-of-use water disinfection system with improved anti-biofouling properties. *RSC Adv.* **2021**, *11*, 4873–4882. [[CrossRef](#)]
40. Zirehpour, A.; Rahimpour, A.; Shamsabadi, A.A.; Gh, M.S.; Soroush, M. Mitigation of thin-film composite membrane biofouling via immobilizing nano-sized biocidal reservoirs in the membrane active layer. *Environ. Sci. Technol.* **2017**, *51*, 5511–5522. [[CrossRef](#)]
41. Dong, C.; Wang, Z.; Wu, J.; Wang, Y.; Wang, J.; Wang, S. A green strategy to immobilize silver nanoparticles onto reverse osmosis membrane for the enhanced anti-biofouling property. *Desalination* **2017**, *401*, 32–41. [[CrossRef](#)]
42. Guillen, G.R.; Pan, Y.; Li, M.; Hoek, E.M.V. Preparation, and characterization of membranes formed by nonsolvent induced phase separation: A review. *Ind. Eng. Chem. Res.* **2011**, *50*, 3798–3817. [[CrossRef](#)]
43. Sánchez-Márquez, J.A.; Fuentes-Ramírez, R.; Cano-Rodríguez, I.; Gamiño-Arroyo, Z.; Rubio-Rosas, E.; Kenny, J.M.; Rescignano, N. Membrane Made of Cellulose Acetate with Polyacrylic Acid Reinforced with Carbon Nanotubes and Its Applicability for Chromium Removal. *Int. J. Polym. Sci.* **2015**, *2015*, 1–12. [[CrossRef](#)]
44. Yadav, N.; Hakkarainen, M. Degradable or not? Cellulose acetate is a model for the complicated interplay between structure, environment, and degradation. *Chemosphere* **2021**, *265*, 128731. [[CrossRef](#)]
45. Tahazadeh, S.; Karimi, H.; Mohammadi, T.; Emrooz, H.B.M.; Tofighy, M.A. Fabrication of biodegradable cellulose acetate/MOF-derived porous carbon nanocomposite adsorbent for methylene blue removal from aqueous solutions. *J. Solid-State Chem.* **2021**, *299*, 122180. [[CrossRef](#)]
46. Unal, I.; Egri, S. Biosynthesis of silver nanoparticles using the aqueous extract of *Rheum ribes*, characterization and the evaluation of its toxicity on HUVECs and *Artemia salina*. *Inorg. Nano-Met. Chem.* **2022**, *23*, 1–4. [[CrossRef](#)]
47. Ferdous, Z.; Nemmar, A. Health impact of silver nanoparticles: A review of the biodistribution and toxicity following various routes of exposure. *Int. J. Mol. Sci.* **2020**, *21*, 2375. [[CrossRef](#)]
48. Gudikandula, K.; Charya Maringanti, S. Synthesis of silver nanoparticles by chemical and biological methods and their antimicrobial properties. *J. Exp. Nanosci.* **2016**, *11*, 714–721. [[CrossRef](#)]

49. Gohil, J.M.; Choudhury, R.R. Introduction to nanostructured and nano-enhanced polymeric membranes: Preparation, function, and application for water purification. In *Nanoscale Materials in Water Purification*; Elsevier: Amsterdam, The Netherlands, 2019; pp. 25–57. [[CrossRef](#)]
50. Sharma, V.K.; Siskova, K.M.; Zboril, R.; Gardea-Torresdey, J.L. Organic-coated silver nanoparticles in biological and environmental conditions: Fate, stability, and toxicity. *Adv. Colloid Interface Sci.* **2014**, *204*, 15–34. [[CrossRef](#)]
51. Trinh, V.T.; Nguyen, T.M.P.; Van, H.T.; Hoang, L.P.; Nguyen, T.V.; Ha, L.T.; Vu, X.H.; Pham, T.T.; Quang, N.V.; Nguyen, X.C. Phosphate adsorption by silver nanoparticles-loaded activated carbon derived from tea residue. *Sci. Rep.* **2020**, *10*, 3634. [[CrossRef](#)] [[PubMed](#)]
52. Zhu, X.; Bai, R.; Wee, K.H.; Liu, C.; Tang, S.-L. Membrane surfaces immobilized with ionic or reduced silver and their anti-biofouling performances. *J. Membr. Sci.* **2010**, *363*, 278–286. [[CrossRef](#)]
53. Zhang, M.; Zhang, K.; De Gussemme, B.; Verstraete, W. Biogenic silver nanoparticles (bio-Ag0) decrease biofouling of bio-Ag0/PES nanocomposite membranes. *Water Res.* **2012**, *46*, 2077–2087. [[CrossRef](#)]
54. Yorseng, K.; Siengchin, S.; Ashok, B.; Rajulu, A.V. Nanocomposite egg shell powder with in situ generated silver nanoparticles using inherent collagen as reducing agent. *J. Bioresour. Bioprod.* **2020**, *5*, 101–107. [[CrossRef](#)]
55. World Health Organization. *Silver in Drinking Water: Background Document for Development of WHO Guidelines for Drinking-Water Quality*; (No. WHO/HEP/ECH/WSH/2021.7); World Health Organization. Available online: <https://www.who.int/westernpacific/publications-detail/WHO-HEP-ECH-WSH-2021.7> (accessed on 1 September 2022).